

Zone plate design for generating annular-focused beams*

Yong Chen(陈勇), Lai Wei(魏来), Qiang-Qiang Zhang(张强强),
Quan-Ping Fan(范全平), Zu-Hua Yang(杨祖华), and Lei-Feng Cao(曹磊峰)[†]

Science and Technology on Plasma Physics Laboratory, Research Center of Laser Fusion,
China Academy of Engineering Physics, Mianyang 621900, China

(Received 6 March 2020; revised manuscript received 20 May 2020; accepted manuscript online 18 June 2020)

Annular-focused beams have attracted attention because of their novel properties and applications in optical trapping, high resolution microscopy, and laser-induced periodic surface structuring. Generation of this beam is very important and necessary. In this article, a novel design of zone plate for forming the annular-focused beams is proposed. The design principle is introduced, and the characteristics of zone plate are analyzed by numerical simulation. The result shows that the zone plate can form a monochromatic ring-shaped intensity distribution in the focal plane. And the design method is also generally suitable for designing the other optical elements to generate the annular-focused beams.

Keywords: zone plate, diffractive optical elements, annular focused beam, laser-induced periodic surface structuring

PACS: 42.25.Fx, 42.79.Ci

DOI: 10.1088/1674-1056/ab9de4

1. Introduction

The fabrication of nanostructures on surfaces is of paramount importance in nanotechnology and materials science.^[1–5] Recently, exploiting the small Gaussian focusing beam, laser-induced periodic surface structuring (LIPSS) has successfully stitched the nanostructures seamlessly with ~ 1 -nm long-range uniformity on bulk and thin films.^[6–8] However, due to the small size of the laser beam (≤ 10 wavelengths) and the scanning speed (≤ 10 $\mu\text{m/s}$), it is much too slow to induce large-size grating structures with the step-and-scan fashion. According to the step-and-scan fashion, the radial scan method based on annular focused beams will increase the efficiency greatly. By continuously changing the radius of the annular focused beam, nanostructures can be created sequentially, with existing structures creating new structures.

Various approaches have been demonstrated to generate annular focused beams, such as axicon-lens, intra-cavity method, crystal fibre, ring-focusing mirror, *etc.*^[9–16] According to the methods above, special structure design of zone plate can also generate annular beams. It has advantages of simplicity, availability, convenience. And combining with the spatial light modulator,^[17] a focal ring with arbitrary radius will be obtained without fabricating any elements. Yu *et al.* proposed the concept of Dammann zone plate^[18,19] and Ma *et al.* proposed the Fresnel–Dammann zone plate,^[20] which can generate a series of annular beams. However, their advantage is equal-intensity multi-beam parallel optical manipulation, while LIPSS needs only one annular focused beam because of the nonlinear feedback mechanisms,^[6] Hidaka,^[21]

Zhang *et al.*,^[22] and Sabatyan^[23] proposed a similar specific structure of Fresnel zone plate, changing the focus from a spot to the ring-shape. But whether the phase-shifted method or the shifting-rotating method, they all designed only one structure of zone plate that the area of inner zones is smaller than that of outer zones. Actually, we also proposed a zone plate design independently, and two different structures were designed. One is the same as what was mentioned above, and the other one is just the opposite that the area of outer zone is smaller than that of inner zone. Compared with the former structure, the latter can suppress the central diffraction intensity and focus sidelobe obviously. In this paper, we design a zone plate to generate ring-shaped focus and simulate the light field energy distribution by scalar diffraction theory based on the two different structures. Furthermore, in order to use the zone plate in the LIPSS, the diffraction properties with different object-image distances and wavelengths are simulated.

2. Principle of design

Figure 1 shows a schematic diagram of the concept of the ring focal zone plate. As is well known, a classic Fresnel zone plate (FZP) that is shown in Fig. 1(a) is a combination of a series of concentric rings and concentrates the light in a similar fashion to a conventional refractive lens. Its one-dimensional structure is shown in Fig. 1(b), and it is so designed that the optical path lengths for the light deflected from adjacent zones toward a common focal point differ by an integral multiple of a design wavelength. If x_n denotes the distance between the n -th structure and the axis, f denotes the focal length, this

*Project supported by the National Key Research and Development Program of China (Grant No. 2017YFA0206004), the National Natural Science Foundation of China (Grant No. 11375160), and the Science and Technology Fund from the Plasma Physics Laboratory, China (Grant No. ZY2018-01).

[†]Corresponding author. E-mail: leifeng.cao@caep.cn

condition is expressed mathematically as

$$x_n^2 + f^2 = \left(f + \frac{n\lambda}{2}\right)^2. \quad (1)$$

The amplitude of a diffracted plane wave in the focal plane of structure in Fig. 1(b) was simulated and calculated. Figure 1(c) shows the normalized intensity profile of the diffracted wave in the focal plane. It is clearly evident that a single focal spot has been achieved.

Transfer the one-dimensional structure by d in the direction perpendicular to the primary axis, and take another side

to be symmetric, then we are able to obtain Fig. 1(e) and

$$(x'_n + d)^2 + f^2 = \left(f + \frac{n\lambda}{2}\right)^2, \quad (2)$$

where x'_n denotes the distance between the n -th structure and the symmetry axis. If d value is positive, the width of the successive outward zones will be gradually increased-then-decreased as seen in the upper of Fig. 1(e), exactly unlike the structure of classic FZP, but like that in Refs. [21–23]. And if d value is negative, the width will behave exactly like FZP as seen in the lower of Fig. 1(e). This is our unique design.

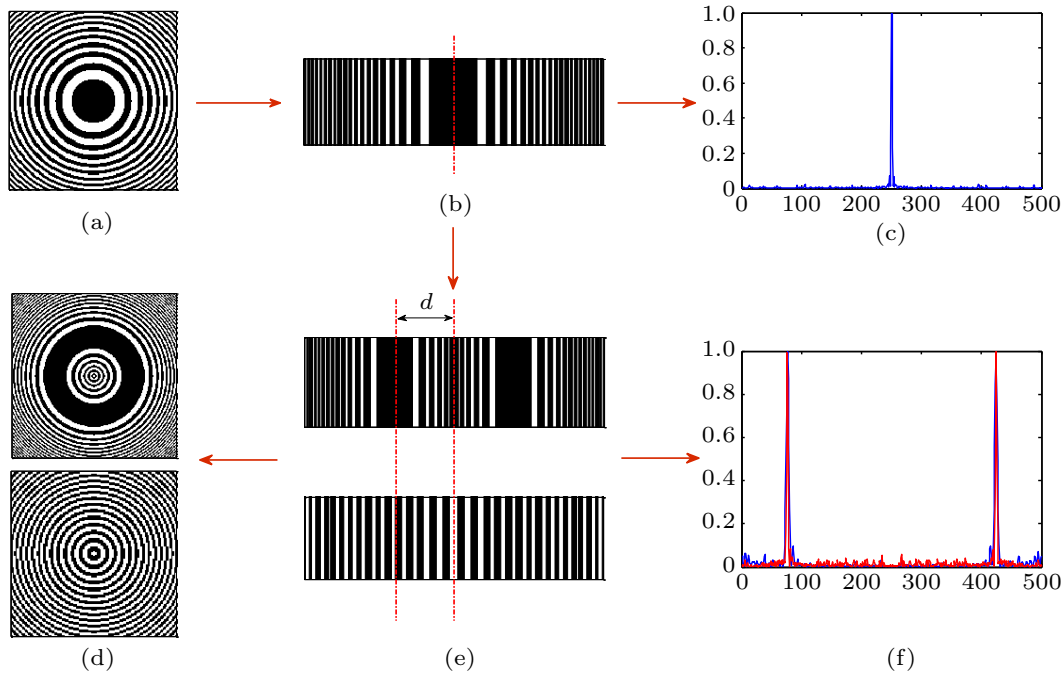


Fig. 1. Schematic diagram of concept of novel zone plate, showing (a) classic FZP, (b) linear FZP, and (c) its simulation results, (d) ring focal zone plate, (e) one-dimensional structure, and (f) its simulation results.

Amplitude of a diffracted plane wave in the focal plane of the structure in Fig. 1(e) was simulated and calculated similarly. Figure 1(f) shows the normalized intensity profile of the diffracted wave in the focal plane. It is clearly evident that two focal spots with a distance of $2d$ have been achieved.

Rotate the structure around the symmetry axis, then we will obtain Fig. 1(d) and have

$$\left(\sqrt{x^2 + y^2} + d\right)^2 + f^2 = \left(f + \frac{n\lambda}{2}\right)^2. \quad (3)$$

Equation (3) is similar to those in Refs. [21–23]. In general, our method and the methods described in Refs. [21–23] can be used to design the structures similar to zone plate structures of Eq. (3) by the direct structures or phases. They are essentially identical. But compared with them, our method is very comprehensive. We consider both positive d and negative d , while they all ignored the condition of negative d . Moreover, our method is easy to understand, and can be directly applied

to the design of other optical elements.

3. Numerical simulations

In the following, to corroborate the analytical results we perform a numerical simulation by using Kirchoff diffraction formula. Amplitude of a diffracted wave $U(x, y, z)$ of wavelength λ at a certain propagation distance z from an object denoted by a pupil function $P(x', y', z')$ can be expressed as convolution term

$$U(x, y, z) = \frac{2\pi e^{ikz}}{i\lambda z} \left\{ P(x, y) \otimes \exp\left[\frac{ik}{2z}(x^2 + y^2)\right] \right\}, \quad (4)$$

where \otimes and $\exp\left[\frac{ik}{2z}(x^2 + y^2)\right]$ denote the convolution operator and free space response function, respectively.

Firstly, we define the ring focal zone plate. The focal length is 50 mm for a wavelength of 632.8 nm. The plate is composed of a large number of square base elements. The

size is $6\ \mu\text{m} \times 6\ \mu\text{m}$, which is similar to the spatial light modulator pixel pitch. As a result, the minimum width of zone is $6\ \mu\text{m}$. Figure 2 shows the microstructures of the zone plates with different ring focal radii. Because of the pixel size, the strips are meander lines. As a result, it will result in some errors. The structures with positive d are the same as those in Refs. [21–23], while the structures with negative d are our

unique design. In order to compare and analyze the two different structures, the zone plates with the same ring focal radius had the same size. We considered the following four cases: (i) the radius is smaller than half of the plate size; (ii) the radius is close to half of the plate size, and (iii) the radius is bigger than half of the plate size, and (iv) the radius is bigger than the plate size.

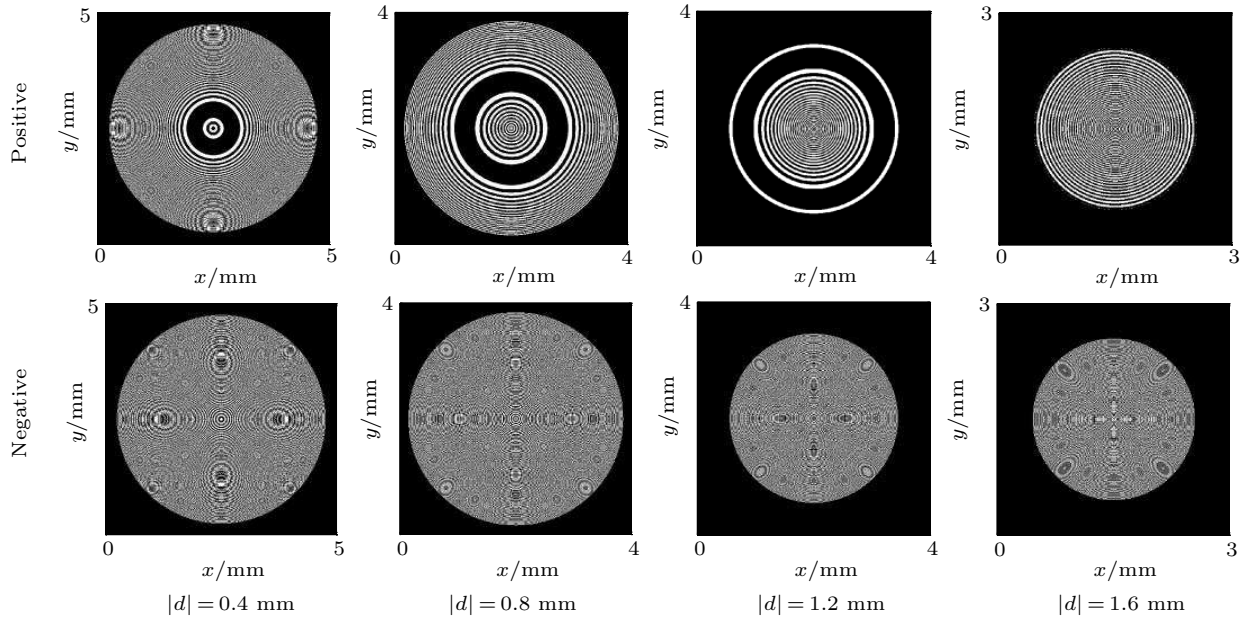


Fig. 2. Structures of ring focal zone plates with different values of d .

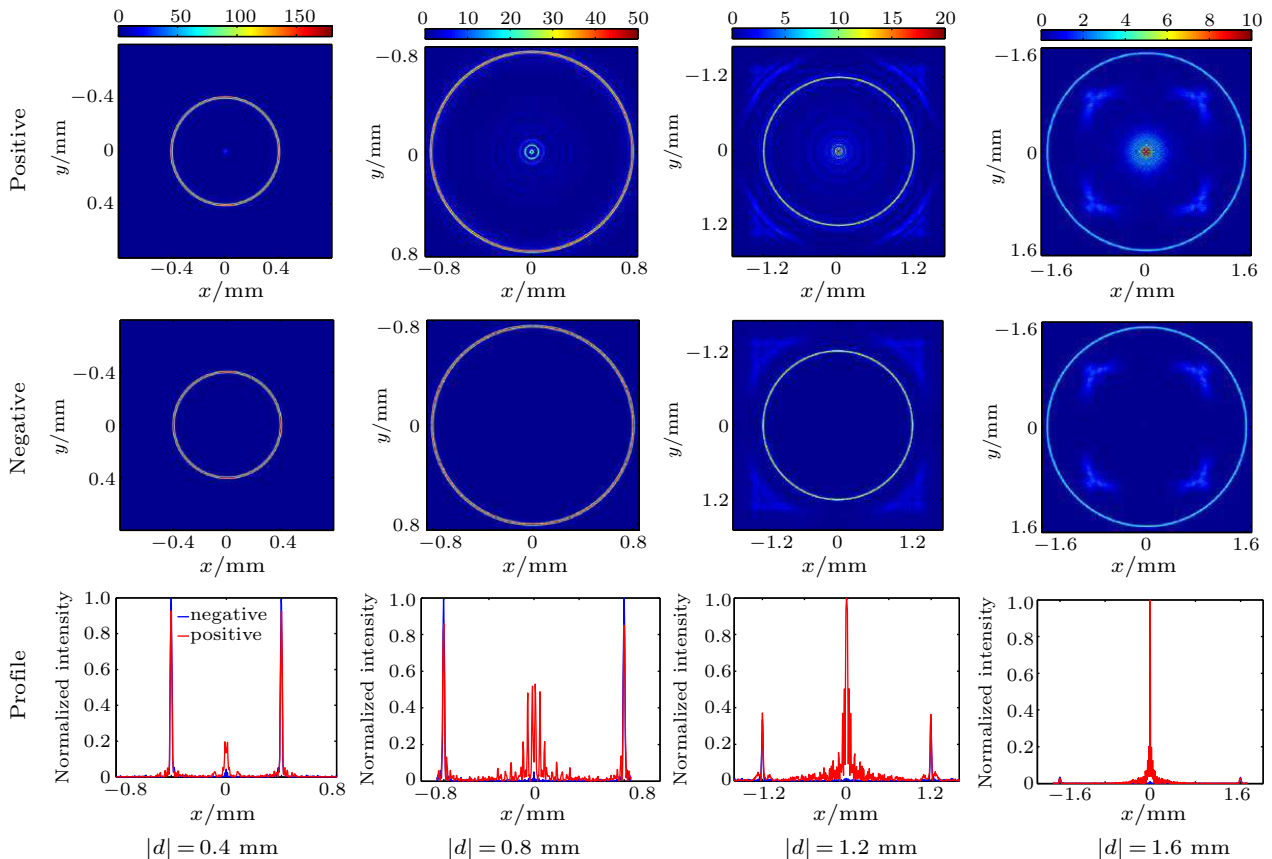


Fig. 3. Energy distributions and intensity profiles of ring focus with different values of d .

To examine the focusing properties of the proposed model and compare the performances of two structures, simulations were performed by considering Eq. (4). Amplitude of a diffracted plane wave in the focal plane was simulated and calculated. Figure 3 shows the light field energy distribution and intensity profile of ring focal spot with different values of d . It is clearly evident that the focal spot is a ring, and the radius coincides well with the theoretical design. And the results with positive d coincide well with those in Refs. [22,23], too. There is another relatively weak focal spot in the focal plane center of both positive structure and negative structure. However, in Fig. 1(f) which is the result of one-dimensional structure, there does not exist a similar phenomenon. So, the relatively weak spot may come from the superposition of the integrals of diffraction in the zones. In the LIPSS, the integrals can be prevented from being superposed by using a high-pass filter. A comparison between the positive structure and the negative structure reveals that the negative structure can suppress the central diffraction intensity and the ring focus sidelobe obviously. In the state of same size, the performance of negative structure is better than that of the positive structure.

In Fig. 3, there exists a relatively weak focal spot in the center. It indicates that it may be independent of wavelength, and the zone plate can form an extra micro-focus broadband modulated source by polychromatic light illumination. In order to demonstrate the inference, we performed the simulations with structure $d = -0.6$ mm and the wavelengths of 532 nm, 632.8 nm, and 800 nm. Figure 4 shows the results. It reveals that the plate can form a monochromatic focal ring and a micro-focus broadband modulated source in the focal plane, which corresponds to the predictions. It is a distinctive characteristic, but the related applications need exploring. Figures 4(a) and 4(b) show the light field energy distribution and intensity profile, respectively. Besides the micro-focus, the 532 nm is mainly distributed inside the focal ring, and the 800 nm is mainly distributed outside the ring. In the micro-focus, the intensity of 632.8 nm is the highest, and the 800 nm is the lowest. The intensity of the focal ring is about 2.8 times that of micro-focus. Moreover, we performed the simulation of the wavelength response properties of the micro-focus, which can be seen in Fig. 5. It rapidly increases and then decreases with wavelength increasing and it peaks at 421 nm. It fluctuates significantly at wavelength less than 531 nm, by comparison, it just obtain slight fluctuation at wavelength more than 531 nm. It indicates that the negative structure has both focusing function and attenuation function.

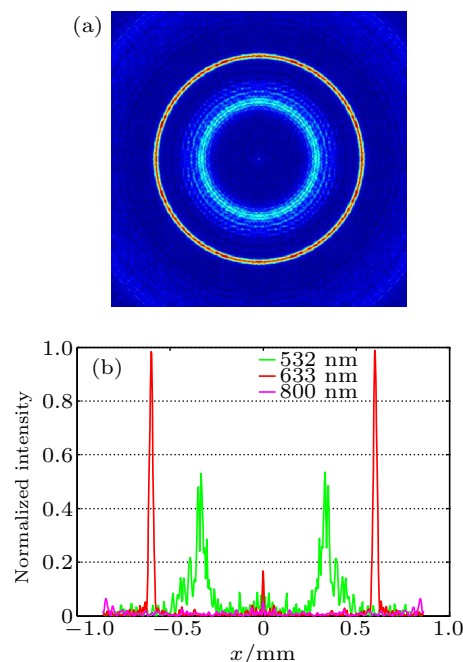


Fig. 4. (a) Energy distribution and (b) intensity profiles of ring focus for three different wavelengths.

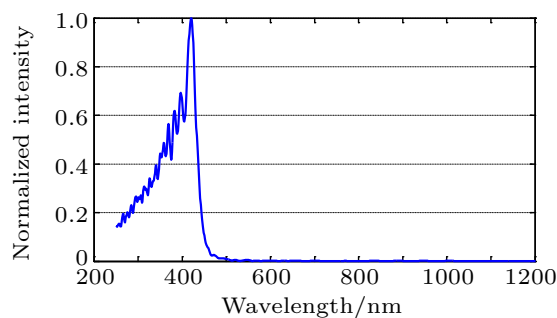


Fig. 5. Wavelength-dependent normalized intensity of micro-focus.

4. Conclusions

In this paper, we introduced a ring focal zone plate and analyzed its focusing performance. It can form a ring focal spot in the focal plane and a micro-focus broadband modulated source under the polychromatic light illumination. Therefore, an annular-focused beam with continuous changing radius can be produced. This will be useful in LIPSS because of the great increasing of the fabrication efficiency. And this design method will be generally suitable for designing the lens and mirrors which can produce annular-focused beams.

References

- [1] Daniel D, Timonen J V, Li R, Velling S J, Kreder M J, Tetreault A and Aizenberg J 2018 *Phys. Rev. Lett.* **120** 244503
- [2] Guay J M, Lesina A C, Cote G, Charron M, Poitras D, Ramunno L, Berini P and Weck A 2017 *Nat. Commun.* **8** 16095
- [3] Zhu S and Wu J 2011 *Chin. Phys. B* **20** 067901
- [4] Liu X W, Meng C, Xu X C, Tang M W, Pang C L and Yang Q 2018 *Chin. Phys. B* **27** 118704
- [5] Jiang Q Q, Li W X, Tang C C, Chang Y C, Hao T T, Pan X Y, Ye H T, Li J J and Gu C Z 2016 *Chin. Phys. B* **25** 118105

- [6] Oktem B, Pavlov I, Ilday S, Kalaycioglu H, Rybak A, Yavas S, Erdogan M and Ilday F O 2013 *Nat. Photon.* **7** 897
- [7] Tokel O, Turnali A, Makey G, Elahi P, Colakoglu T, Ergecen E, Yavuz O, Hubner R, Borra M Z, Pavlov I, Bek A, Turan R, Kesim D K, Tozburun S, Ilday S and Ilday F O 2017 *Nat. Photon.* **11** 639
- [8] Pavlov I A, Rybak A S, Dobrovolskiy A M, Kadan V M, Blonskiy I V, Ilday F O, Kazantseva Z I and Gvozдовskyy I A 2018 *J. Mol. Liq.* **267** 212
- [9] Lin J, Wei M, Liang H, Lin K and Hsieh W 2007 *Opt. Express* **15** 2940
- [10] Sun Q G, Zhou K Y, Fang G Y, Liu Z J and Liu S T 2012 *Chin. Phys. B* **21** 014208
- [11] Esseling M, Alpmann C, Schnelle J, Meissner R and Denz C 2018 *Sci. Rep.* **8** 5029
- [12] Ozeri R, Khaykovich L and Davidson N 1999 *Phys. Rev. A* **59** 1750
- [13] Tung J C, Ma Y Y, Miyamoto K, Chen Y F and Omatsu T 2018 *Sci. Rep.* **8** 16576
- [14] Boyko O, Planchon T A, Mercere P, Valentin C and Balcou P 2005 *Opt. Commun.* **246** 131
- [15] Zhang M Y, Li S G, Yao Y Y, Fu B and Zhang L 2010 *Chin. Phys. B* **19** 047103
- [16] Mimura H, Takeo Y, Motoyama H, Senba Y, Kishimoto H and Ohashi H 2019 *Appl. Phys. Lett.* **114** 131101
- [17] Ren Z J, He J P and Shi Y L 2018 *Chin. Phys. B* **27** 124201
- [18] Yu J J, Zhou C H, Jia W, Cao W G, Wang S Q, Ma J Y and Cao H C 2012 *Appl. Opt.* **51** 1619
- [19] Yu J J, Zhou C H, Jia W, Hu A D, Cao W G, Wu J and Wang S Q 2012 *Appl. Opt.* **51** 6799
- [20] Ma Y Y, Ye C C, Ke J, Zhang J Y, Zhu J Q and Ling Z Q 2016 *Appl. Opt.* **55** 7218
- [21] Hidaka T 1991 *Jpn. J. Appl. Phys.* **30** 1738
- [22] Zhang C C, Hu Y L, Li J W, Li G Q, Chu J R and Huang W H 2014 *Opt. Express* **22** 3983
- [23] Sabatyan A and Meshginqalam B 2014 *Appl. Opt.* **53** 5995